Qiang Cao,[1] Xin Cui,[1] Rui Wu,[1] Lin Zha,[1] Xianfeng Wang,[2] John S. Parks,[3] Liqing Yu,[4] Hang Shi,[1] and Bingzhong Xue[1]

Myeloid Deletion of α1AMPK Exacerbates Atherosclerosis in LDL Receptor Knockout (LDLRKO) Mice

Diabetes 2016;65:1565–1576 | DOI: 10.2337/db15-0917

Macrophage inflammation marks all stages of atherogenesis, and AMPK is a regulator of macrophage inflammation. We therefore generated myeloid α1AMPK knockout (MAKO) mice on the LDL receptor knockout (LDLRKO) background to investigate whether myeloid deletion of α1AMPK exacerbates atherosclerosis. When fed an atherogenic diet, MAKO/LDLRKO mice displayed exacerbated atherosclerosis compared with LDLRKO mice. To determine the underlying pathophysiological pathways, we characterized macrophage inflammation/chemotaxis and lipid/cholesterol metabolism in MAKO/LDLRKO mice. Myeloid deletion of α1AMPK increased macrophage inflammatory gene expression and enhanced macrophage migration and adhesion to endothelial cells. Remarkably, MAKO/LDLRKO mice also displayed higher composition of circulating chemotaxically active Ly-6C^{high} monocytes, enhanced atherosclerotic plaque chemokine expression, and monocyte recruitment into plaques, leading to increased atherosclerotic plaque macrophage content and inflammation. MAKO/LDLRKO mice also exhibited higher plasma LDL and VLDL cholesterol content, increased circulating apolipoprotein B (apoB) levels, and higher liver apoB expression. We conclude that macrophage α1AMPK deficiency promotes atherogenesis in LDLRKO mice and is associated with enhanced macrophage inflammation and hypercholesterolemia and that macrophage α1AMPK may serve as a therapeutic target for prevention and treatment of atherosclerosis.

Inflammatory processes mark all stages of atherogenesis, from early endothelial activation to eventual rupture of atherosclerotic plaque (1–3). Experimental interventions aimed at reducing inflammation are atheroprotective, whereas removing or blocking anti-inflammatory molecules (i.e., interleukin [IL]-10 or transforming growth factor-β) accelerates atherosclerosis (1). Arterial wall macrophage accumulation is a key feature of atherosclerosis development (4,5) that is initiated with monocyte chemotaxis into atheroma. Monocytes expressing the chemokine (C-C motif) receptor 2 (CCR2) migrate to activated endothelial cells that secrete monocyte chemoattractant protein 1 (MCP1) and adhere to the injured endothelial cells by vascular cell adhesion molecule 1 (6–10). Within the intima, monocytes mature into macrophages, which accelerate atherosclerotic formation by producing proinflammatory cytokines, the accumulation of cholesterol, and foam cell formation (1,2). Selective depletion of monocytes/macrophages by diphtheria treatment in a transgenic mouse model expressing a CD11b-driven diphtheria toxin receptor in monocyte/macrophages provides resistance to atherosclerosis (11). Accumulating evidence strongly supports the notion that macrophage inflammation is a key component of atherosclerosis. Therefore, understanding how macrophage inflammation/function is altered in deregulated metabolic conditions with excess nutrients (e.g., cholesterol, fatty acids, and glucose) may provide novel mechanisms and therapeutic targets in the prevention and treatment of atherosclerosis. As such, AMPK, a cellular nutrient and energy sensor, has generated interest due to its anti-inflammatory function.

AMPK is an evolutionarily conserved cellular energy sensor that regulates metabolic pathways in lipid, cholesterol,

[1]Department of Biology and Center for Obesity Reversal, Georgia State University, Atlanta, GA
[2]Department of Internal Medicine, Wake Forest School of Medicine, Winston-Salem, NC
[3]Section on Molecular Medicine, Department of Internal Medicine, Wake Forest School of Medicine, Winston-Salem, NC
[4]Department of Animal and Avian Sciences, University of Maryland, College Park, MD
Corresponding authors: Hang Shi, hshi3@gsu.edu, and Bingzhong Xue, bxue@gsu.edu.

Received 3 July 2015 and accepted 31 December 2015.
This article contains Supplementary Data online at http://diabetes.diabetesjournals.org/lookup/suppl/doi:10.2337/db15-0917/-/DC1.

See accompanying article, p. 1493.

and glucose metabolism (12). We (13) and others (14,15) have shown that activating macrophage AMPK significantly suppresses inflammation induced by lipopolysaccharide (LPS) and free fatty acid (FFA), which is exerted primarily through the α1AMPK isoform in macrophages. Therefore, AMPK may serve as an energy sensor linking nutrient metabolism to the regulation of inflammatory signaling (13). Other studies also reported that AMPK activation suppresses macrophage proliferation induced by oxidized LDL (16). However, whether the anti-inflammatory function of AMPK protects against atherosclerosis is still not clear. For example, administration of the AMPK activator 5-aminoimidazole-4-carboxymide-1-β-D-ribofuranoside (AICAR) to apolipoprotein (apo)$E^{-/-}$ mice prevents atherosclerosis development (17). However, the pleiotropic functions of AMPK in multiple tissues have made it difficult to understand whether and to what extent macrophage AMPK expression protects against atherosclerosis. This study was therefore designed to directly investigate the role of macrophage α1AMPK in the atherosclerosis development through the generation of myeloid-specific α1AMPK knockout (MAKO) mice on the genetic background of LDL receptor knockout (MAKO/LDLRKO). These MAKO/LDLRKO mice and their littermate controls (floxed [fl/fl]/LDLRKO) were fed an atherogenic diet for 16 weeks, followed by quantification of *1)* atherosclerosis extent; *2)* in vitro macrophage inflammation and chemotaxis; *3)* macrophage content, inflammation, and chemotaxis in the atherosclerotic aortic lesions; and *4)* plasma lipid/cholesterol profile.

RESEARCH DESIGN AND METHODS

Mice

α1AMPK fl/fl mice were provided by Dr. Sean Morrison at The University of Texas Southwestern Medical School (18). Lysozyme $Cre^{+/-}$ (Lyz-Cre) (19) and LDLRKO mice (20) were purchased from The Jackson Laboratory (Bar Harbor, ME). The fl/fl mice were crossed with Lyz-Cre mice to generate the MAKO mice. MAKO mice were further bred with LDLRKO to generate MAKO/LDLRKO mice with myeloid-specific deletion of α1AMPK on the genetic background of LDLRKO. Eight-week-old MAKO/LDLRKO and their littermate control fl/fl/LDLRKO mice (eight mice/group) were fed an atherogenic diet containing 42% calories from fat and 0.2% (wt/wt) cholesterol for 16 weeks (Research Diets D12079B). Body weight was monitored weekly. All animal procedures were approved by the Georgia State University Institutional Animal Care and Use Committee.

To study insulin sensitivity, 6-week-old MAKO and their littermate control fl/fl mice (eight mice/group) were fed a high-fat (HF) diet containing 60% of calories from fat (Research Diets D1249) for 16 weeks to establish diet-induced obesity. Blood glucose was measured with an OneTouch Ultra Glucose Meter (LifeScan, Mulpitas, CA), and insulin was measured by a rat insulin ELISA kit (Crystal Chem, Downers Grove, IL). Plasma adiponectin was also measured by an ELISA kit (Crystal Chem). Glucose tolerance tests (GTTs) and insulin tolerance tests (ITTs) were conducted as we previously described (21,22).

Quantification of Atherosclerosis

Atherosclerosis development was evaluated as described previously (23). Briefly, mice were killed after 4 h of food removal. The circulatory system was perfused with PBS before the heart and aorta were removed. The upper one-third of the heart was dissected and embedded in optimal cutting temperature compound (Sakura Tissue-Tek, Torrance, CA), frozen, and stored at −80°C. Blocks were serially cut at 8-μm intervals and stained with hematoxylin and 0.5% Oil Red O (Sigma-Aldrich) to evaluate aortic sinus atherosclerotic intimal area. Atherosclerotic lesion area and Oil Red O–positive area were quantified using Image-Pro Plus software (Media Cybernetics, Bethesda, MD). Three sections of staining were quantified for each mouse, and eight mice per group were used in each cohort we studied.

The whole aorta (from the sinotubular junction to the iliac bifurcate) was dissected and fixed in 10% formalin, and the adventitia was cleaned. Aortas were opened along the longitudinal axis and pinned onto black silicon elastomer (Rubber-Cal, Santa Ana, CA) for the quantification of atherosclerotic lesion area. The percentage of total aortic surface covered with atherosclerotic lesions was quantified by Image-Pro Plus software.

Plasma Lipid Analysis

Mice were fasted for 4 h prior to euthanization. Blood was collected to analyze plasma lipid and cholesterol profiles, as described previously (23). Briefly, plasma total cholesterol (TC) (Pointe Scientific, Canton, MI), free cholesterol (FC) (Wako, Richmond, VA), and triglyceride (TG) (Wako) concentrations were measured using enzymatic assays according to the manufacturer's instructions. Cholesterol ester (CE) was calculated by multiplying the difference between TC and FC by 1.67 (24). Plasma lipoproteins were separated by size using fast protein liquid chromatography, and cholesterol distribution among lipoprotein fractions was determined by enzymatic cholesterol assays.

Cell Culture

To isolate bone marrow–derived macrophages (BMDMs), bone marrow was flushed from the femur and tibia, dispersed, and cultured in DMEM containing 20% FBS and 30% L929 conditional medium for 5–7 days. Peritoneal macrophages were isolated by lavage 5 days after an intraperitoneal injection of 3% thioglycolate solution (Difco; BD Biosciences, San Jose, CA). Cells were stimulated with 10 ng/mL LPS for 4 h, and mRNA expression levels were measured by quantitative real-time RT-PCR.

Cholesterol Efflux to ApoA-I or HDL

Macrophage cholesterol efflux to apoA-I or HDL was measured as described previously (23). Briefly, BMDMs were isolated from MAKO/LDLRKO and their littermate control fl/fl/LDLRKO mice as described above. Cells were incubated with 1 μCi/mL [^{3}H]-cholesterol in the presence

of 50 μg/mL acetylated LDL (Kalen Biomedical, Montgomery Village, MD) for 24 h. Cells were washed and equilibrated for 2 h in medium with lipid-free BSA. HDL- or apoA-I–mediated cholesterol efflux was performed by adding HDL or apoA-I for an additional 24 or 4 h, respectively. Radioactivity was measured in medium and cell lysates. Cholesterol efflux was calculated as radioactivity in the medium divided by the sum of radioactivity in medium and cell lysate.

Cholesterol Content in Peritoneal Macrophages

Peritoneal macrophages were isolated from MAKO/LDLRKO and their fl/fl/LDLRKO littermate controls fed an atherogenic diet for 16 weeks, as described above. Cells were plated at 1×10^6/well in six-well plates for 2 h and washed, and lipid was extracted with isopropanol. Cellular cholesterol content was measured as we previously described (23).

Hepatic Lipid Measurement

Liver lipid extraction was conducted as previously described with minor modifications (25). Briefly, ~100 mg of liver was thawed, minced, and weighed in a glass tube, and 3 mL $CHCl_3$:MeOH (2:1) was added to the samples to extract lipid at room temperature overnight. The samples were further washed with $CHCl_3$:MeOH (2:1) twice, and the combined solvent extracts were dried at 60°C. Three milliliters of $CHCl_3$:MeOH (2:1) and 0.6 mL 0.05% H_2SO_4 were added into tubes, and the phases were separated by 2,000 revolutions per minute centrifugation for 15 min. An aliquot of the bottom phase was dried down. The lipid extraction was dissolved in 2% Triton X-100 and used for TG quantification using a L-Type TG M test (Wako Chemicals). The data were normalized to liver weight.

Immunoblotting

Immunoblotting was performed as described previously (23). SDS-PAGE was run with 2 μL plasma, and goat–anti-human apoB antibody (1:1,000; Academy Bio-Medical Co.) was used to detect apoB protein levels.

Immunohistochemistry

Sections of aortic sinus were immunostained with the following primary antibodies: rat monoclonal antibody against CD68 (Clone FA11, 1:75; AbD Serotec, Raleigh, NC), followed by staining with alkaline phosphatase-conjugated mouse anti-rat (for CD68, 1:50) secondary antibodies (Jackson ImmunoResearch Laboratories, West Grove, PA). Control slides contained no primary antibody. The CD68-positive areas were analyzed using Image-Pro Plus software.

Flow Cytometry Analysis

Immune cell composition analysis was conducted using flow cytometry as previously described (23). Briefly, peripheral blood (100 μL) was obtained from atherogenic diet–fed MAKO/LDLRKO mice and their littermate controls (fl/fl/LDLRKO), and red blood cells were lysed using the ammonium-chloride-potassium (ACK) lysis buffer (Lonza, Allendale, NJ). The remaining white blood cells were incubated with the following antibodies: PE-CF594-CD45 (BD Horizon), PE-Cy5.5-CD4 (BD Pharmingen), APC-Cy7-CD8 (BD Pharmingen), Pacific Blue-CD19 (BD Horizon), PE-Cy7-CD11b (BD Pharmingen), APC-CD115 (eBioscience), and PerCP-Cy5.5-Ly-6C (BD Pharmingen). Data were acquired with FACS using BD FACS Fortessa and analyzed using FlowJo software.

Total RNA Isolation From the Whole Aorta, Aortic Macrophages, and Quantitative RT-PCR

For chemokine expression in aortas, the whole aortas (from the sinotubular junction to the iliac bifurcation) were dissected and immediately frozen in liquid nitrogen. Total RNA was extracted using the TRI Reagent kit (Molecular Research Center, Cincinnati, OH), and gene expression was assessed by quantitative RT-PCR using ABI Universal PCR Master Mix (Applied Biosystems, Foster City, CA) using a Stratagene Mx3000p thermocycler (Stratagene, La Jolla, CA). Cyclophilin was used to normalize the gene expression data. The primer and probe sets used in the assays were purchased from Applied Biosystems/Life Technologies (Grand Island, NY).

For gene expression in aortic macrophages, the digested aortas were used to isolate macrophages with rat anti-mouse F4/80 antibodies (AbD Serotec), followed by a pull down of F4/80-positive cells with sheep anti-rat microbeads using a magnetic-activated cell sorting system (Miltenyi Biotec, Auburn, CA), as described previously (22,23). The isolated F4/80-positive aortic macrophages were used for RNA extraction with TRI Reagent (Molecular Research Center) and gene expression analysis as described above (22,23).

Blood Monocyte Labeling and Quantification of Monocyte Recruitment Into Intima

Ly-$6C^{high}$ (Ly-$6C^{hi}$) monocytes were labeled as described previously (26). Briefly, MAKO/LDLRKO and their littermate control fl/fl/LDLRKO mice were injected with 250 μL clodronate-liposome through the retro-orbital venous sinus to deplete blood monocytes. Eighteen hours later, 250 μL diluted 1.0 μm Fluoresbrite Yellow Green Microspheres (1:4 diluted with PBS) were injected into the bloodstream of mice to label Ly-$6C^{hi}$ monocytes. After 24 h, blood was drawn to determine the percentage of bead-positive monocytes each mouse. The aortic sinus was dissected 3 days after injection to quantify the number of intimal beads, as described previously (26).

Macrophage Migration and Adhesion Assay

Macrophage migration and adhesion assay was performed as described previously (23). Macrophage migration assay was performed using a CytoSelect 96-Well Cell Migration Assay kit (Cell Biolabs, San Diego, CA) according to the manufacturer's instructions. Briefly, BMDMs (1.5×10^5/well) were plated in the membrane chamber, which was placed on top of the feeder tray. Cells were incubated with 10 ng/mL MCP1 at 37°C for 20 h. Migrated cells were dissociated from the membrane, lysed, and quantified using CyQUANT GR fluorescent dye with a Victor 3 plate reader (PerkinElmer, Waltham, MA).

BMDM adhesion assays were conducted with a CytoSelect Leukocyte-endothelium Adhesion Assay kit (Cell Biolabs) according to the manufacturer's instructions. Briefly, human microvascular endothelial cells, adult dermis (HMVECad)

(Invitrogen, Carlsbad, CA) were seeded at 6×10^4/well in a 96-well plate overnight. BMDMs were labeled with LeukoTracker dye for 1 h at 37°C and incubated with a monolayer of the HMVECad cells, which were pretreated with 10 ng/mL tumor necrosis factor-α (TNF-α) for 6 h. Wells were washed 1 h after incubation, and adherent macrophages were lysed. The fluorescent signal from each well was measured with a Victor 3 plate reader (PerkinElmer).

Statistics

All data are expressed as mean ± SEM. Differences between groups were analyzed for statistical significance by *t* test or one- or two-way ANOVA, as appropriate.

RESULTS

Myeloid Deletion of α1AMPK Exacerbates the Development of Atherosclerosis in LDLRKO Mice

To study the role of macrophage α1AMPK in the development of atherosclerosis, we generated MAKO/LDLRKO mice as described in RESEARCH DESIGN AND METHODS. The α1AMPK mRNA and protein levels in BMDMs isolated from MAKO/LDLRKO mice were decreased by 82% and 60% (Supplementary Fig. 1*A–C*), respectively, compared with littermate controls. Similar suppression of α1AMPK mRNA and protein levels was also observed in peritoneal macrophages isolated from MAKO/LDLRKO mice (Supplementary Fig. 1*D–F*). Moreover, we found that the inhibition of α1AMPK mRNA and protein in BMDMs isolated from MAKO/LDLRKO mice also significantly suppressed the basal phosphorylation of αAMPK and acetyl-CoA carboxylase (ACC), a direct downstream target of AMPK (Supplementary Fig. 2*A*). Further, the activated phosphorylation of αAMPK and ACC by AICAR, a specific agonist of AMPK, was also substantially blocked in BMDMs with α1AMPK deficiency (Supplementary Fig. 2*B*). These data suggest that myeloid deletion of α1AMPK downregulates AMPK signaling in macrophages. We next determined whether the myeloid deletion of α1AMPK affects the AMPK expression and signaling in other key metabolic tissues, such as liver, fat, and skeletal muscle, due to potential leakiness of the Cre expression in those tissues. We found, however, that myeloid deletion of α1AMPK did not change α1AMPK expression in liver, fat, and skeletal muscle and that the myeloid deficiency of α1AMPK did not alter the AMPK signaling, including the phosphorylation of αAMPK and ACC in those tissues (Supplementary Fig. 3). These data suggested that the α1AMPK deletion is likely restricted to myeloid lineage cells.

Eight-week-old MAKO/LDLRKO and their littermate control fl/fl/LDLRKO mice were fed an atherogenic diet containing 42% calories from fat and 0.2% (wt/wt) cholesterol for 16 weeks. Because previous studies reported that the expression of macrophage α1AMPK was suppressed by inflammatory stimuli such as LPS and FFAs (13) and by obesity (15), we therefore determined whether myeloid deletion of α1AMPK by the genetic approach can further decrease the supposedly lower macrophage α1AMPK by feeding of an atherogenic diet. Indeed, we still observed an 80% reduction of α1AMPK mRNA in peritoneal macrophages isolated from MAKO/LDLRKO mice compared with their littermate control fl/fl/LDLRKO mice fed the atherogenic diet for 16 weeks (Supplementary Fig. 4*A*). Similarly, a comparable inhibition of α1AMPK mRNA was also observed in macrophages isolated from the aortas of MAKO/LDLRKO mice fed the atherogenic diet (Supplementary Fig. 4*B*).

Myeloid deletion of α1AMPK did not alter body weight (Supplementary Fig. 4*C*) or liver and fat pad mass (Supplementary Fig. 4*D*). However, myeloid deletion of α1AMPK significantly increased the atherosclerotic lesions in intimal areas of aortic roots by 38% (Fig. 1*A* and *B*) and also enhanced the atherosclerotic surface lesion areas in the whole aorta by 63% (Fig. 1*C* and *D*) compared with the control mice.

Myeloid Deletion of α1AMPK Increases Macrophage Inflammation and Infiltration Into Atherosclerotic Plaques

Macrophage inflammation is a key component in atherosclerosis development (2). We (13) and others (14) have reported that α1AMPK is a negative regulator of macrophage inflammation. We therefore examined whether myeloid deletion of α1AMPK worsens atherosclerosis by promoting macrophage inflammation and chemotaxis. Indeed, we found in this study that macrophage α1AMPK deficiency substantially promoted LPS or interferon-γ–stimulated expression of proinflammatory genes, such as TNF-α, IL-6, IL-1β, MCP1, and inducible nitric oxide synthase (iNOS), in primarily cultured BMDMs isolated from MAKO mice (Fig. 2*A–E*). To test whether macrophage α1AMPK deficiency also affects macrophage function, we performed macrophage adhesion and chemotaxis assays with BMDMs isolated from MAKO/LDLRKO mice. We found that α1AMPK deficiency increased macrophage adhesion to endothelial cells and enhanced the ability of macrophages to migrate toward an MCP1 gradient (Fig. 2*F* and *G*).

We then determined whether the enhanced macrophage inflammation and chemotaxis induced by α1AMPK deficiency affected atherosclerotic plaque macrophage content. Using immunohistochemistry, we stained macrophages in aortic sinus sections with anti-CD68 antibodies and found that atherosclerotic plaque macrophage content was higher in MAKO/LDLRKO mice compared with the control mice (Fig. 3). Interestingly, we found that the expression of genes involved in chemotaxis, such as MCP1, chemokine (C-X-C motif) ligand 1 (CXCL1), CXCL2, intercellular adhesion molecule 1, and vascular cell adhesion molecule, was significantly increased in aortas isolated from MAKO/LDLRKO mice compared with that of control mice (Fig. 4*A*), suggesting that the increased production of chemokines in the atherosclerotic plaques may attract monocyte infiltration. We also determined the content of T cells in the whole aortas. We found that the expression of T-cell markers did not change in the aortas isolated from MAKO/LDLRKO and their

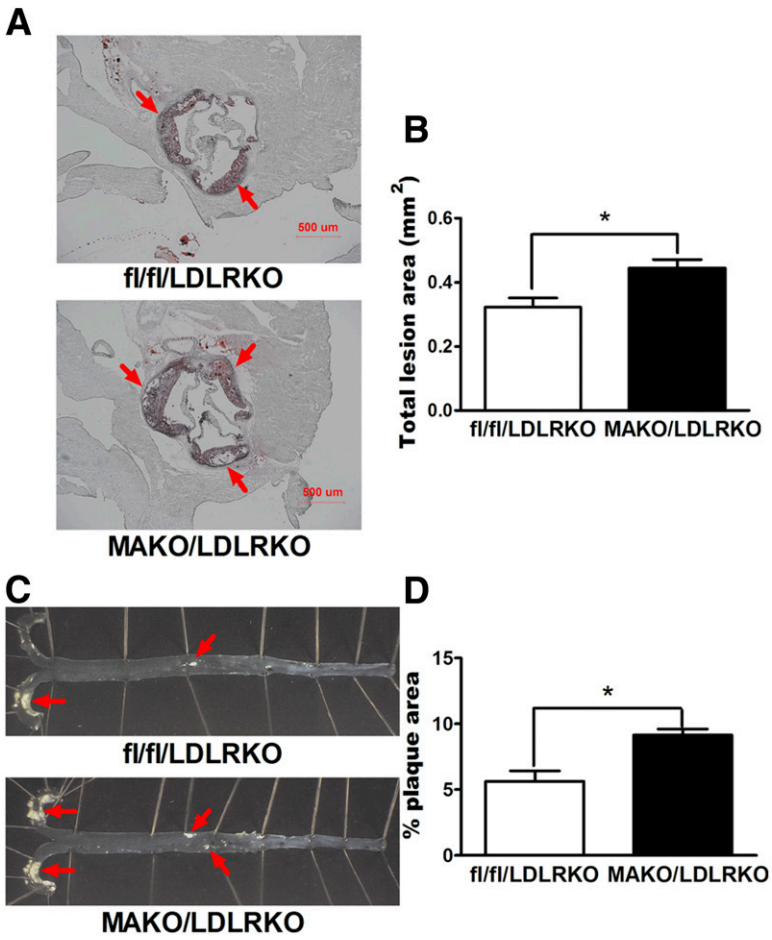

Figure 1—Myeloid deletion of α1AMPK exacerbates the atherosclerosis development in MAKO/LDLRKO mice. *A*: A representative cross-sectional image of aortic sinus stained with Oil Red O. The lesion areas are indicated by red arrows. *B*: Quantification of the lesion areas. *C*: Representative images of aortic surface lesions. The atherosclerotic plaques are indicated by red arrows. *D*: Aortic surface lesion area normalized to total aortic surface area. *B* and *D*: Data are expressed as mean ± SEM ($n = 8$). *$P < 0.05$ vs. fl/fl/LDLRKO control. Eight-week old male MAKO/LDLRKO and control mice were fed an atherogenic diet for 16 weeks. Quantitation of atherosclerosis was conducted as described in RESEARCH DESIGN AND METHODS.

littermate control mice (Supplementary Fig. 5), suggesting that T-cell infiltration was not involved in the development of atherosclerosis in MAKO/LDLRKO mice. To determine the inflammatory status of macrophages infiltrated in the atherosclerotic plaques, we isolated macrophages from the plaques and measured the expression of inflammatory genes. We found that the expression of proinflammatory cytokines, such as TNF-α, IL-1β, MCP1, and the inflammasome marker NLR family pyrin domain containing 3 (NLRP3), was significantly upregulated in macrophages isolated from atherosclerotic plaques of MAKO/LDLRKO mice (Fig. 4*B*). Ly-6C^{hi} monocytes are a subset of circulating monocytes that infiltrate into inflammatory sites, including atherosclerotic lesions (27,28). Using FACS analysis, we examined this particular monocyte subpopulation and found that the percentage of Ly-6C^{hi} monocytes was increased in overall circulating monocytes of MAKO/LDLRKO mice, whereas the composition of Ly-6C^{low} monocytes was decreased accordingly (Fig. 5*A*). However, we did not detect any differences in the composition of major immune cell types in blood between MAKO/LDLRKO mice and control mice, including monocytes, CD4$^+$ and CD8$^+$ T cells, and CD19$^+$ B cells (Supplementary Fig. 6). To further test the ability of in vivo migration of α1AMPK-deficient macrophages, we performed in vivo monocyte recruitment to intima in MAKO/LDLRKO and control mice. We found that macrophage α1AMPK deficiency markedly increased monocyte migration to the intima of MAKO/LDLRKO mice (Fig. 5*B* and *C*).

Myeloid Deletion of α1AMPK Causes Hypercholesterolemia

Another important risk factor for the development of atherosclerosis is hypercholesterolemia (29). Interestingly, MAKO/LDLRKO mice exhibited hyperlipidemia and hypercholesterolemia evident by increased plasma TG, TC, and CE levels, as well as FFA levels (Fig. 6*A* and *B*), compared with control mice. In addition, increased plasma cholesterol content in both VLDL and LDL was observed in MAKO/LDLRKO mice, whereas the HDL

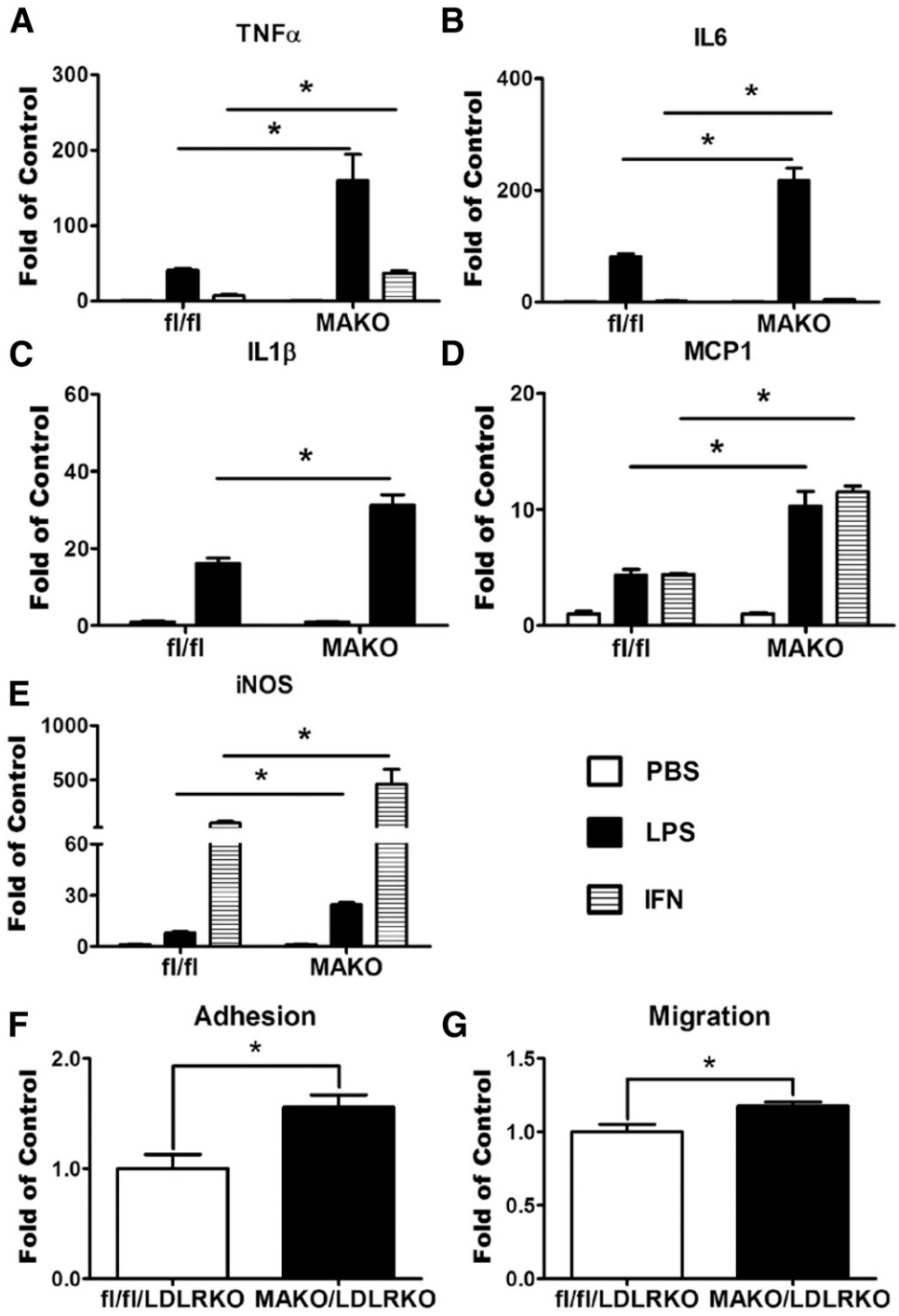

Figure 2—Macrophage α1AMPK deficiency increases macrophage inflammation and chemotaxis. Macrophage α1AMPK deficiency promotes the expression of proinflammatory genes, including TNF-α (*A*), IL-6 (*B*), IL-1β (*C*), MCP1 (*D*), and iNOS (*E*). Macrophage α1AMPK deficiency enhances macrophage adhesion to endothelial cells (*F*) and migration (*G*). Gene expression was measured by real-time RT-PCR and normalized to cyclophilin. Macrophage adhesion and migration were conducted as described in RESEARCH DESIGN AND METHODS. Data are expressed as mean ± SEM (n = 6–8). fl/fl, fl/fl/LDLRKO; IFN, interferon. *$P < 0.05$ vs. fl/fl/LDLRKO control.

cholesterol concentration was without change (Fig. 6*C* and *D*). Because apoB100 is a major structural apo in VLDL and LDL particles and is important for VLDL and LDL production, we measured the abundance of this apo in plasma. Immunoblotting analysis showed higher plasma apoB100 and apoB48 protein levels in MAKO/LDLRKO mice than in control mice fed an atherogenic diet for 10 weeks and 16 weeks (Fig. 6*E–G* and Supplementary Fig. 7). We also found that hepatic apoB mRNA levels (Fig. 7*A*) and protein expression (Fig. 7*B*) were increased in MAKO/LDLRKO mice compared with the control mice. Because inflammation is one of the factors

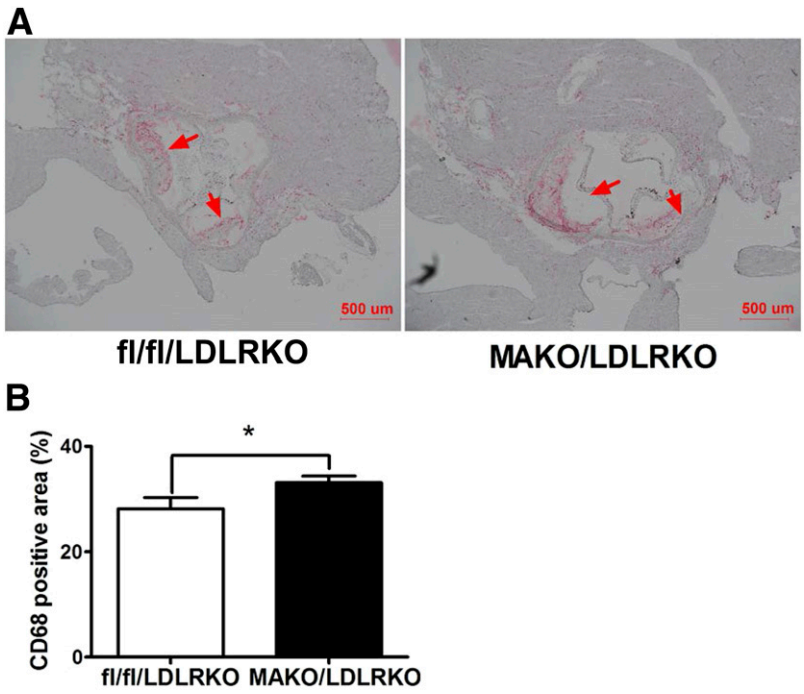

Figure 3—Macrophage α1AMPK deficiency increases macrophage content in atherosclerotic plaques of MAKO/LDLRKO mice. *A*: Representative images of aortic sinus stained with CD68 antibody. *B*: Quantification of CD68-positive lesion areas. Male MAKO/LDLRKO and control mice (8 weeks old) were fed an atherogenic diet for 16 weeks. The upper one-third of the heart was dissected and embedded in optimal cutting temperature compound, cryosectioned at 8 μmol/L intervals, and stained with anti-CD68 antibodies. Data are expressed as mean ± SEM (n = 6–8). *P < 0.05 vs. fl/fl/LDLRKO control.

that have been shown to increase apoB expression (30,31), we examined the hepatic inflammatory status of MAKO/LDLRKO mice. Real-time quantitative RT-PCR analysis revealed that the expression of proinflammatory genes, such as TNF-α, IL-1β, MCP1, and iNOS, was upregulated in the liver of MAKO/LDLRKO mice fed an atherogenic diet (Fig. 7*C*). However, we did not observe changes in hepatic TG, TC, FC, and CE content in MAKO/LDLRKO mice fed an atherogenic diet (Supplementary Fig. 8).

Macrophages play a critical role in the development of atherosclerosis by accumulating lipid and cholesterol to form lipid-laden foam cells (29). However, we found that macrophage α1AMPK deficiency did not change the content of TC, CE, and FC accumulation in peritoneal macrophages isolated from MAKO/LDLRKO mice fed the atherogenic diet (Supplementary Fig. 9*A*). In addition, MAKO/LDLRKO and control mice had similar expression of macrophage genes involved in cholesterol metabolism and transport, such as liver X receptor α (LXR-α), ATP-binding cassette, subfamily A, member 1 (ABCA1), and ATP-binding cassette, subfamily G, member 1 (ABCG1) (Supplementary Fig. 9*B*), and genes involved in fatty acid oxidation, such as carnitine palmitoyltransferase 1a (CPT1), cytochrome c oxidase subunit I (COX1), peroxisome proliferative–activated receptor γ coactivator 1 α (PGC1-α), PGC1-β, and acyl-CoA oxidase 1 (ACOX1) (Supplementary Fig. 9*C*). Finally, macrophage α1AMPK deficiency had no effect on cholesterol efflux to apoA-I and to HDL (Supplementary Fig. 9*D*).

Myeloid Deletion of α1AMPK Does Not Affect Insulin Sensitivity in MAKO/LDLRKO Mice Fed an Atherogenic Diet but Causes Insulin Resistance in MAKO Mice Fed an HF Diet

Since Galic et al. (15) reported that disruption of macrophage AMPK signaling by AMPK-β1 knockout through bone marrow transplantation exacerbates obesity-induced inflammation and insulin resistance, we therefore determined whether myeloid deletion of α1AMPK would affect insulin sensitivity in MAKO/LDLRKO mice. Fed the atherogenic diet containing 42% of fat and 0.2% (wt/wt) of cholesterol for 16 weeks, MAKO/LDLRKO mice had no changes in insulin sensitivity evident by normal GTTs, ITTs, and fed insulin levels compared with their littermate controls (Supplementary Fig. 10*A*–*C*), and they did not show any difference in circulating adiponectin levels (Supplementary Fig. 10*D*). To more carefully examine the potential effect of macrophage α1AMPK on obesity-induced insulin resistance, we also generated another mouse model with myeloid deletion of α1AMPK on the C57BL/6J background, in which the intact LDL receptor (LDLR) gene was preserved. α1AMPK fl/fl mice were crossed with Lyz-Cre mice to generate MAKO mice. MAKO and their littermate control fl/fl mice were fed a standard HF diet containing 60% of calories from fat,

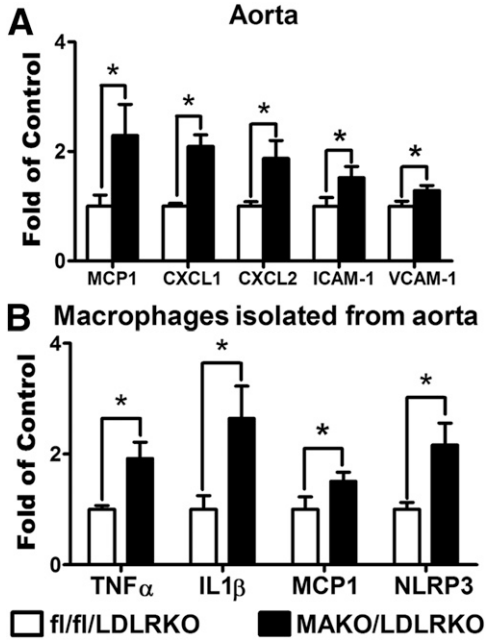

Figure 4—Myeloid deletion of α1AMPK increases chemokine expression in aortas and macrophage inflammation in atherosclerotic plaques. *A*: Myeloid deletion of α1AMPK increases chemokine expression in aortas. ICAM-1, intercellular adhesion molecule 1; VCAM-1, vascular cell adhesion molecule 1. *B*: Macrophage α1AMPK deficiency increases the expression of proinflammatory genes in macrophages of atherosclerotic plaques in MAKO/LDLRKO and control mice fed an atherogenic diet. *A*: The whole aortas were dissected and used for total RNA extraction. Gene expression was measured by real-time RT-PCR and normalized to cyclophilin. *B*: The aorta macrophages were isolated using a magnetic-activated cell sorting system as described in RESEARCH DESIGN AND METHODS. Data are expressed as mean ± SEM (n = 8). *P < 0.05 vs. fl/fl/LDLRKO control.

which we have successfully used to induce diet-induced obesity and insulin resistance (21,22). There was no difference in body weight between MAKO and the control fl/fl mice (Supplementary Fig. 11*A*). However, MAKO mice displayed a phenotype of glucose intolerance assessed by GTTs and insulin resistance assessed by ITTs (Supplementary Fig. 11*B* and *C*) with enhanced blood insulin levels (Supplementary Fig. 11*D*), whereas there was no difference in blood adiponectin levels (Supplementary Fig. 11*E*). This was associated with increased expression of proinflammatory cytokine IL-6 and TNF-α in adipose tissue of MAKO mice fed the HF diet (Supplementary Fig. 12).

DISCUSSION

The current study was designed to address the hypothesis that macrophage α1AMPK negatively regulates the development of atherosclerosis by dampening inflammation. The plausibility of this hypothesis derives from several prior observations. First, macrophage inflammation plays a key role in the development of atherosclerosis and is involved in all stages of atherogenesis, including atheroma formation, progression, and rupture (1,2,23). Second, we (13) and others (14) (15) have shown that α1AMPK is a negative regulator of macrophage inflammation. Whether the anti-inflammatory function of α1AMPK protects against atherogenesis is not clear, however. To address this question, we generated mice with myeloid-specific deletion of α1AMPK in the LDLRKO background and investigated diet-induced atherosclerosis progression. We found that myeloid deficiency of α1AMPK markedly promotes atherosclerosis development. To examine the underlying pathophysiological changes, we investigated macrophage inflammation/chemotaxis and lipid/cholesterol metabolism.

Because macrophage inflammation plays a key role in the development of atherosclerosis (1,2), we first determined whether α1AMPK deficiency worsened macrophage inflammation/chemotaxis, contributing to atherosclerosis development in MAKO/LDLRKO mice. AMPK is an evolutionarily conserved serine/threonine kinase and has been viewed as a metabolic sensor or fuel gauge that monitors cellular AMP and ATP levels (12). Activation of AMPK represses ATP-consuming anabolic pathways (e.g., fatty acid and cholesterol synthesis) and induces ATP-producing catabolic pathways (e.g., fatty acid oxidation) (12). Thus, AMPK is a key signaling molecule that integrates hormonal and nutrient signals to regulate metabolic pathways. Recently, we (13) and others (14) have shown that macrophage AMPK activation prevents LPS- and FFA-induced proinflammatory cytokine expression and nuclear factor-κB signaling, indicating that AMPK is an important negative regulator of macrophage inflammation (13). The anti-inflammatory function of macrophage AMPK might be mediated by upregulation of SIRT1 expression and activity (13,21). SIRT1 can subsequently deacetylate the nuclear factor-κB subunit p65, leading to downregulation of macrophage inflammation (13,32). Moreover, Galic et al. (15) demonstrated that inhibiting macrophage AMPK signaling by AMPK-β1 deletion reduces fatty acid oxidation and increases diacylglycerol accumulation, leading to enhanced expression of proinflammatory markers. With this in mind, the inhibition of fatty acid oxidation caused by AMPK deficiency may increase accumulation of fatty acids in macrophages, leading to endoplasmic reticulum stress that may further activate inflammatory response (33,34). Downregulation of macrophage AMPK may also mediate fatty acid activation of NLRP3 inflammasome, resulting in IL-1β production (35,36). In sum, macrophage AMPK controls multiple pathways in regulation of the inflammatory network.

AMPK may therefore be the potential link between nutrient metabolism and inflammation. Indeed, we showed that AICAR, an AMPK activator, reduces obesity-induced insulin resistance through inhibiting macrophage inflammation (21). As such, macrophage AMPK activation becomes a very attractive target for treatment of insulin resistance. A report from the Steinberg group showed that hematopoietic AMPK-β1 deficiency worsens obesity-induced

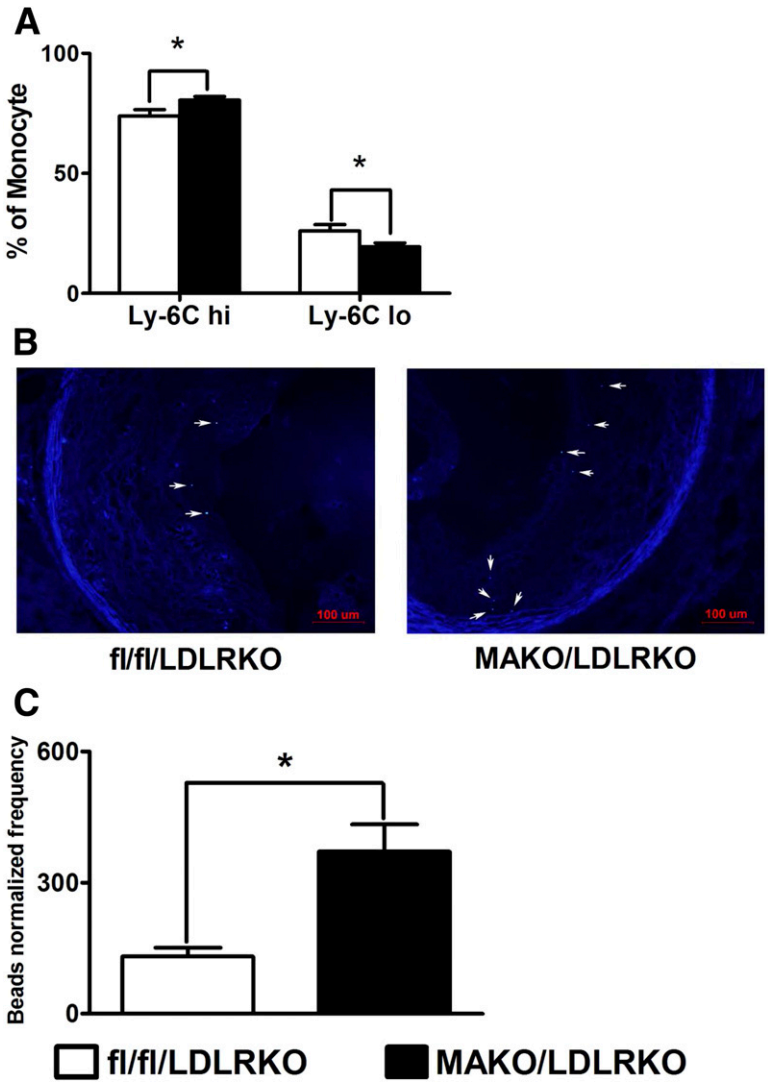

Figure 5—Myeloid deletion of α1AMPK increases the percentage of Ly-C6^{hi} monocytes in circulation and monocyte trafficking to atherosclerotic plaques. *A*: Myeloid deletion of α1AMPK increases the percentage of Ly-C6^{hi} monocytes in circulation. *B* and *C*: Myeloid deletion of α1AMPK increases monocyte trafficking to atherosclerotic plaques. *B*: Representative cross-sectional images of aortic sinus with fluorescent bead-labeled macrophages (arrows). *C*: Quantification of fluorescent bead number in intima normalized by the labeled circulating monocytes. Leukocyte composition and monocyte traffic analyses were conducted as described in RESEARCH DESIGN AND METHODS. Data are expressed as mean ± SEM (n = 8). *P < 0.05 vs. fl/fl/LDLRKO control.

inflammation and insulin resistance (15). Activation of AMPK by AICAR also decreases atherosclerosis in apoE$^{-/-}$ mice (17). However, pleiotropic AMPK activation by AICAR in multiple metabolic tissues has made it difficult to determine the specific role of macrophage AMPK in insulin resistance and atherosclerosis. Additional genetic studies involving deletion of AMPK in specific tissues are required to separate the systemic effects on energy metabolism from the direct anti-inflammatory effects and to determine the extent to which the anti-inflammatory effects of AMPK alter atherosclerosis progression. Our current study provides in vitro and in vivo evidence that myeloid deletion of α1AMPK promotes macrophage inflammation and chemotaxis (adhesion and migration) and increases macrophage infiltration into atherosclerotic plaques, which likely contributes to exacerbated atherosclerosis in MAKO/LDLRKO mice. Interestingly, we have previously shown that AMPK signaling is downregulated by inflammatory stimuli and in nutrient-rich conditions, such as exposure to LPS and FFAs, and in diet-induced obesity (13). Downregulation of macrophage AMPK in obesity, which is characterized by excess nutrient intake and chronic inflammation (e.g., increased circulating cytokine levels), may result in exaggerated macrophage inflammation and chemotaxis that worsens atherosclerosis development.

We also found that MAKO/LDLRKO mice exhibit increased plasma TG, FFA, TC, and CE concentrations and that the increased cholesterol was confined to the

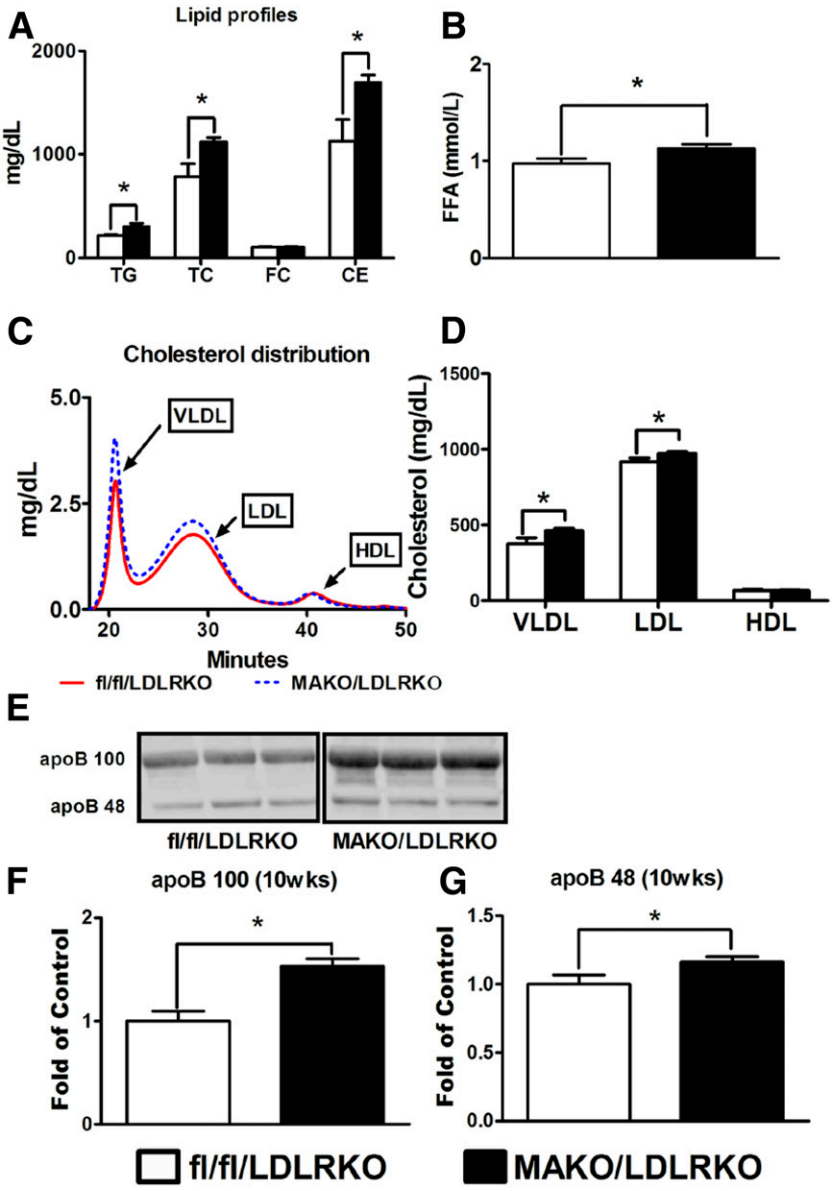

Figure 6— Myeloid deletion of α1AMPK causes hyperlipidemia in MAKO/LDLRKO mice. Myeloid deletion of α1AMPK increases plasma TG, TC, and CE levels (*A*), as well as FFA levels (*B*). *C* and *D*: Myeloid deletion of α1AMPK increases VLDL and LDL cholesterol concentration. *C*: A representative lipoprotein cholesterol distribution determined after fast protein liquid chromatography fractionation of plasma. *D*: Quantitation of cholesterol content distributed in VLDL, LDL, and HDL. *E*–*G*: Myeloid deletion of α1AMPK increases plasma apoB100 and apoB48. *A*–*D*: Male MAKO/LDLRKO and control mice (8 weeks old) were fed an atherogenic diet for 16 weeks. Plasma lipid and cholesterol profiles were analyzed as described in RESEARCH DESIGN AND METHODS. *E*–*G*: Male 8-week-old MAKO/LDLRKO and control mice were fed an atherogenic diet for 10 weeks. Plasma apoB protein content was measured using immunoblotting. Data are expressed as mean ± SEM (n = 6–8). *P < 0.05 vs. fl/fl/LDLRKO control. wks, weeks.

atherogenic lipoproteins, LDL, and VLDL. These results suggest that macrophage α1AMPK-deficient mice have increased hepatic lipoprotein production and/or decreased catabolism, leading to hyperlipidemia and increased atherosclerosis relative to control mice. Although the systemic change of the circulating lipid profile was somewhat unexpected, we think that this is not likely due to leakiness of the Cre gene expression in other tissues such as liver. The Lyz-Cre mouse (19) we purchased from The Jackson Laboratory has been extensively used to generate myeloid deletion of genes of interest and has been reported in many publications from other groups (37–40) and our group (21). The Cre construct knocked into the endogenous lysozyme gene locus is faithfully expressed in myeloid lineage cells (19). In fact, we also determined whether the myeloid deletion of α1AMPK affects the AMPK expression and signaling in other key metabolic tissues, such as liver, fat, and skeletal muscle, due to potential leakiness of the Cre

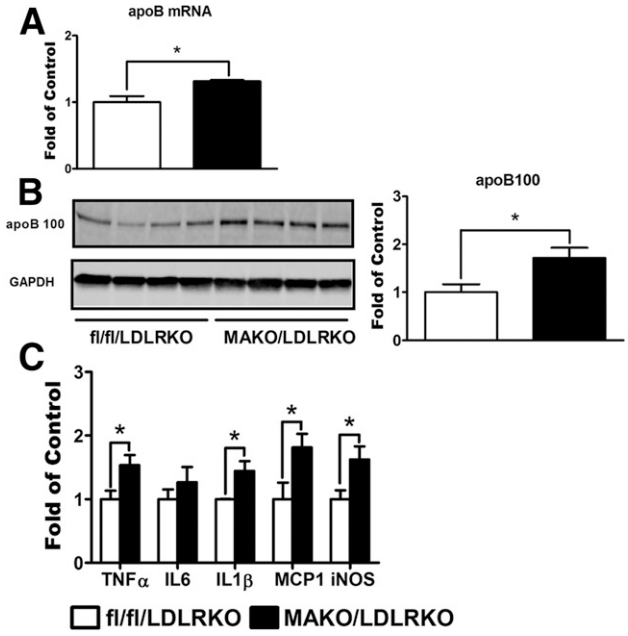

Figure 7—Myeloid deletion of α1AMPK upregulates apoB expression in liver of MAKO/LDLRKO mice. Myeloid deletion of α1AMPK upregulates apoB mRNA (*A*) and protein (*B*). *C*: Myeloid deletion of α1AMPK stimulates the expression of proinflammatory genes in liver. Male 8-week-old MAKO/LDLRKO and control mice were fed an atherogenic diet for 10 weeks. mRNA and protein of gene of interest were measured by real-time RT-PCR and immunoblotting, respectively. Data are expressed as mean ± SEM (n = 6–8). *P < 0.05 vs. fl/fl/LDLRKO control.

expression in those tissues. We found that myeloid deletion of α1AMPK did not change α1AMPK expression in liver, fat, and skeletal muscle and that the myeloid deficiency of α1AMPK did not alter the AMPK signaling in those tissues. Our data suggested that the α1AMPK deletion is likely restricted to myeloid lineage cells. However, to exclude potential leakiness of the Cre expression, other approaches, such as bone marrow transplantation, will be warranted to confirm and will also be complementary to our observation on the protective effect of macrophage α1AMPK in atherosclerosis. Alternatively, it seems plausible that increased macrophage inflammation is responsible for altered hepatic lipid metabolism and increased plasma lipid levels. This idea is supported by published data demonstrating that acute inflammation increases the synthesis of apoB (30,31) and hepatic lipids (41), leading to hyperlipidemia. Although MAKO/LDLRKO mice had no increase in hepatic lipid content relative to control mice, we have previously shown that hepatic lipid content does not necessarily reflect hepatic lipid secretion (42–44). Because macrophage α1AMPK is a negative regulator of macrophage inflammation, hepatic macrophages (e.g., Kupffer cells) without α1AMPK presumably secrete proinflammatory cytokines that contribute to hepatic inflammation, although our results do not rule out the possibility that extrahepatic macrophages may contribute to this phenotype. Nonetheless, additional studies are required to address the causative effect of hepatic inflammation in apoB protein production in our study.

We noted the discrepancy of the phenotype of insulin sensitivity between MAKO/LDLRKO and MAKO mice fed the respective atherogenic diet and the standard HF diet. There are two potential reasons. First, MAKO/LDLRKO and MAKO mice were fed two different diets with different fat contents. MAKO/LDLRKO mice were fed the atherogenic diet containing 42% of calories from fat, and MAKO mice were fed the standard HF diet containing 60% of calories from fat (including lards, a more detrimental type of saturated fat). As a result, the MAKO mice fed the HF diet are more obese than the MAKO/LDLRKO mice, with MAKO mice being ~5 g heavier. In addition to the difference in body weight, the two different diets themselves may cause different metabolic consequences. Second, MAKO/LDLRKO and MAKO mice have different genetic backgrounds. In addition to both lacking myeloid α1AMPK, MAKO/LDLRKO mice have whole-body deletion of LDLR, whereas MAKO mice have the intact LDLR gene. Whether or how the presence or absence of LDLR gene may affect insulin sensitivity is not clear.

In summary, our data demonstrate that myeloid-specific α1AMPK deletion exacerbates atherosclerosis in LDLRKO mice. Myeloid α1AMPK deficiency upregulates macrophage proinflammatory gene expression and enhances macrophage migration and adhesion to endothelial cells, leading to monocyte infiltration into atherosclerotic plaques. MAKO/LDLRKO mice fed the atherogenic diet also display hypercholesterolemia and hyperlipidemia that further exacerbate atherosclerosis progression. We conclude that macrophage α1AMPK is atheroprotective in LDLRKO mice and may serve as a therapeutic target for prevention and treatment of atherosclerosis.

Funding. This work was supported by National Heart, Lung, and Blood Institute grants R01-HL-119962 (J.S.P.) and R01-HL-107500 (B.X.), National Institute of Diabetes and Digestive and Kidney Diseases grants R01-DK-085176 (L.Y.) and R01-DK-084172 (H.S.), American Heart Association grants 11GRNT7370080 (H.S.) and 10SDG3900046 (B.X.), and American Diabetes Association grant 7-13-BS-159 (H.S.).

Duality of Interest. No potential conflicts of interest relevant to this article were reported.

Author Contributions. Q.C., X.C., R.W., L.Z., and X.W. performed most of the experiments. J.S.P. provided technical support on lipid/cholesterol/monocyte traffic/atherosclerosis analyses. J.S.P. and L.Y. contributed to discussion and reviewed and edited the manuscript. Q.C., H.S., and B.X. conceived the hypothesis, designed the study, analyzed the data, and wrote the manuscript. H.S. and B.X. are the guarantors of this work and, as such, had full access to all the data in the study and take responsibility for the integrity of the data and the accuracy of the data analysis.

References

1. Galkina E, Ley K. Immune and inflammatory mechanisms of atherosclerosis. Annu Rev Immunol 2009;27:165–197

2. Libby P, Ridker PM, Hansson GK; Leducq Transatlantic Network on Atherothrombosis. Inflammation in atherosclerosis: from pathophysiology to practice. J Am Coll Cardiol 2009;54:2129–2138

3. de Winther MP, Kanters E, Kraal G, Hofker MH. Nuclear factor kappaB signaling in atherogenesis. Arterioscler Thromb Vasc Biol 2005;25:904–914
4. Rocha VZ, Libby P. Obesity, inflammation, and atherosclerosis. Nat Rev Cardiol 2009;6:399–409
5. Wilson HM, Barker RN, Erwig LP. Macrophages: promising targets for the treatment of atherosclerosis. Curr Vasc Pharmacol 2009;7:234–243
6. Boring L, Gosling J, Cleary M, Charo IF. Decreased lesion formation in CCR2-/- mice reveals a role for chemokines in the initiation of atherosclerosis. Nature 1998;394:894–897
7. Gu L, Okada Y, Clinton SK, et al. Absence of monocyte chemoattractant protein-1 reduces atherosclerosis in low density lipoprotein receptor-deficient mice. Mol Cell 1998;2:275–281
8. Kamei N, Tobe K, Suzuki R, et al. Overexpression of monocyte chemoattractant protein-1 in adipose tissues causes macrophage recruitment and insulin resistance. J Biol Chem 2006;281:26602–26614
9. Kanda H, Tateya S, Tamori Y, et al. MCP-1 contributes to macrophage infiltration into adipose tissue, insulin resistance, and hepatic steatosis in obesity. J Clin Invest 2006;116:1494–1505
10. Weisberg SP, Hunter D, Huber R, et al. CCR2 modulates inflammatory and metabolic effects of high-fat feeding. J Clin Invest 2006;116:115–124
11. Stoneman V, Braganza D, Figg N, et al. Monocyte/macrophage suppression in CD11b diphtheria toxin receptor transgenic mice differentially affects atherogenesis and established plaques. Circ Res 2007;100:884–893
12. Xue B, Kahn BB. AMPK integrates nutrient and hormonal signals to regulate food intake and energy balance through effects in the hypothalamus and peripheral tissues. J Physiol 2006;574:73–83
13. Yang Z, Kahn BB, Shi H, Xue BZ. Macrophage alpha1 AMP-activated protein kinase (alpha1AMPK) antagonizes fatty acid-induced inflammation through SIRT1. J Biol Chem 2010;285:19051–19059
14. Sag D, Carling D, Stout RD, Suttles J. Adenosine 5′-monophosphate-activated protein kinase promotes macrophage polarization to an anti-inflammatory functional phenotype. J Immunol 2008;181:8633–8641
15. Galic S, Fullerton MD, Schertzer JD, et al. Hematopoietic AMPK beta1 reduces mouse adipose tissue macrophage inflammation and insulin resistance in obesity. J Clin Invest 2011;121:4903–4915
16. Ishii N, Matsumura T, Kinoshita H, et al. Activation of AMP-activated protein kinase suppresses oxidized low-density lipoprotein-induced macrophage proliferation. J Biol Chem 2009;284:34561–34569
17. Li D, Wang D, Wang Y, Ling W, Feng X, Xia M. Adenosine monophosphate-activated protein kinase induces cholesterol efflux from macrophage-derived foam cells and alleviates atherosclerosis in apolipoprotein E-deficient mice. J Biol Chem 2010;285:33499–33509
18. Nakada D, Saunders TL, Morrison SJ. Lkb1 regulates cell cycle and energy metabolism in haematopoietic stem cells. Nature 2010;468:653–658
19. Clausen BE, Burkhardt C, Reith W, Renkawitz R, Förster I. Conditional gene targeting in macrophages and granulocytes using LysMcre mice. Transgenic Res 1999;8:265–277
20. Ishibashi S, Brown MS, Goldstein JL, Gerard RD, Hammer RE, Herz J. Hypercholesterolemia in low density lipoprotein receptor knockout mice and its reversal by adenovirus-mediated gene delivery. J Clin Invest 1993;92:883–893
21. Yang Z, Wang X, He Y, et al. The full capacity of AICAR to reduce obesity-induced inflammation and insulin resistance requires myeloid SIRT1. PLoS One 2012;7:e49935
22. Wang X, Yang Z, Xue B, Shi H. Activation of the cholinergic antiinflammatory pathway ameliorates obesity-induced inflammation and insulin resistance. Endocrinology 2011;152:836–846
23. Cao Q, Wang X, Jia L, et al. Inhibiting DNA Methylation by 5-Aza-2′-deoxycytidine ameliorates atherosclerosis through suppressing macrophage inflammation. Endocrinology 2014;155:4925–4938
24. Chapman MJ, Goldstein S, Lagrange D, Laplaud PM. A density gradient ultracentrifugal procedure for the isolation of the major lipoprotein classes from human serum. J Lipid Res 1981;22:339–358
25. Bligh EG, Dyer WJ. A rapid method of total lipid extraction and purification. Can J Biochem Physiol 1959;37:911–917
26. Tacke F, Alvarez D, Kaplan TJ, et al. Monocyte subsets differentially employ CCR2, CCR5, and CX3CR1 to accumulate within atherosclerotic plaques. J Clin Invest 2007;117:185–194
27. Rosas M, Thomas B, Stacey M, Gordon S, Taylor PR. The myeloid 7/4-antigen defines recently generated inflammatory macrophages and is synonymous with Ly-6B. J Leukoc Biol 2010;88:169–180
28. Swirski FK, Libby P, Aikawa E, et al. Ly-6Chi monocytes dominate hypercholesterolemia-associated monocytosis and give rise to macrophages in atheromata. J Clin Invest 2007;117:195–205
29. Lusis AJ. Atherosclerosis. Nature 2000;407:233–241
30. Tsai J, Zhang R, Qiu W, Su Q, Naples M, Adeli K. Inflammatory NF-kappaB activation promotes hepatic apolipoprotein B100 secretion: evidence for a link between hepatic inflammation and lipoprotein production. Am J Physiol Gastrointest Liver Physiol 2009;296:G1287–G1298
31. Aspichueta P, Pérez-Agote B, Pérez S, Ochoa B, Fresnedo O. Impaired response of VLDL lipid and apoB secretion to endotoxin in the fasted rat liver. J Endotoxin Res 2006;12:181–192
32. Schug TT, Xu Q, Gao H, et al. Myeloid deletion of SIRT1 induces inflammatory signaling in response to environmental stress. Mol Cell Biol 2010;30:4712–4721
33. Erbay E, Babaev VR, Mayers JR, et al. Reducing endoplasmic reticulum stress through a macrophage lipid chaperone alleviates atherosclerosis. Nat Med 2009;15:1383–1391
34. Lichtenstein L, Mattijssen F, de Wit NJ, et al. Angptl4 protects against severe proinflammatory effects of saturated fat by inhibiting fatty acid uptake into mesenteric lymph node macrophages. Cell Metab 2010;12:580–592
35. Wen H, Gris D, Lei Y, et al. Fatty acid-induced NLRP3-ASC inflammasome activation interferes with insulin signaling. Nat Immunol 2011;12:408–415
36. Steinberg GR, Schertzer JD. AMPK promotes macrophage fatty acid oxidative metabolism to mitigate inflammation: implications for diabetes and cardiovascular disease. Immunol Cell Biol 2014;92:340–345
37. Seo SW, Koeppen M, Bonney S, et al. Differential tissue-specific function of Adora2b in cardioprotection. J Immunol 2015;195:1732–1743
38. Liu K, Zhao E, Ilyas G, et al. Impaired macrophage autophagy increases the immune response in obese mice by promoting proinflammatory macrophage polarization. Autophagy 2015;11:271–284
39. Vannella KM, Barron L, Borthwick LA, et al. Incomplete deletion of IL-4Rα by LysM(Cre) reveals distinct subsets of M2 macrophages controlling inflammation and fibrosis in chronic schistosomiasis. PLoS Pathog 2014;10:e1004372
40. Gautier EL, Ivanov S, Williams JW, et al. Gata6 regulates aspartoacylase expression in resident peritoneal macrophages and controls their survival. J Exp Med 2014;211:1525–1531
41. Khovidhunkit W, Kim MS, Memon RA, et al. Effects of infection and inflammation on lipid and lipoprotein metabolism: mechanisms and consequences to the host. J Lipid Res 2004;45:1169–1196
42. Brown JM, Chung S, Sawyer JK, et al. Inhibition of stearoyl-coenzyme A desaturase 1 dissociates insulin resistance and obesity from atherosclerosis. Circulation 2008;118:1467–1475
43. Parks JS, Johnson FL, Wilson MD, Rudel LL. Effect of fish oil diet on hepatic lipid metabolism in nonhuman primates: lowering of secretion of hepatic triglyceride but not apoB. J Lipid Res 1990;31:455–466
44. Shewale SV, Boudyguina E, Zhu X, et al. Botanical oils enriched in n-6 and n-3 FADS2 products are equally effective in preventing atherosclerosis and fatty liver. J Lipid Res 2015;56:1191–1205